A Biologically-inspired Wavelength Resource Allocation for Optical Path/Packet Integrated Networks

Shin'ichi Arakawa*, Norimitsu Tsutsui*, and Masayuki Murata*
* Graduate School of Information Science and Technology, Osaka University, Japan
{arakawa,n-tsutsui,murata}@ist.osaka-u.ac.jp

***Abstract*—In this paper, we develop a biologically-inspired wavelength allocation method that allocates wavelengths to path/packet integrated networks. Our method is based on a biological symbiosis model that explains co-existing and co-working of two types of bacterial strains in biological systems. The results show that the biologically-inspired wavelength allocation method achieves a nearly 40% reduction of the latency from a threshold-based dynamic wavelength allocation method.**

***Index Terms*—path/packet integration, IP over WDM, circuit switching, wavelength routing, Transmission Control Protocol (TCP), latency**

I. Introduction

To effectively utilizing the wavelength-routing capability in WDM-based optical networks, two approaches have been investigated [1], [2]. One of approaches is to transfer the data based on the circuit-switching paradigm. That is, when a data transfer request arises at a source node, a wavelength is dynamically reserved between the source and destination nodes. Then, the data is transferred using the allocated wavelength channel. After the data transmission through the wavelength channel, the channel is immediately released. Another approach is called IP-packet over WDM [2] where a data is transferred based on the packet switching paradigm. In this approach, a virtual network topology (VNT) is constructed in advance by setting up lightpaths between two IP routers. The lightpath behaves as the virtual link from viewpoint of IP networks. Then, a data transfer is performed based on the packet switching paradigm over the VNT.

The main strength of the circuit-switching paradigm is that the data request solely uses and enjoys the bandwidth of wavelength channels, which would be attractive for recent multimedia services and/or cloud services that require high reliability and large bandwidth. Another strength is that a congestion avoidance mechanism is no longer necessary. That is, any transport protocols other than TCP can be used for the data transfer. In a recent study, a transport protocol that effectively utilizes the wavelength channel is investigated in Ref. [3]. The drawbacks of this approach are the lightpath setup delay, defined from when data transfer request arises to time when data transfer starts, and blocking during the lightpath establishment.

The current Internet is mainly based on the packet switching paradigm. However, many problems arise with increasing traffic demand and advances of related networking technologies and networking services. For example, the packet drop rate and packet delay increases because of congestion caused by other user traffic [4], which is an inevitable characteristic and may be crucial for services requiring high reliability and large bandwidth. To relax this, over-provisioning of link capacity and router's processing capability are widely used. However, the over-provisioning is eventually difficult because of technological constraints, such as the limitation of packet processing speeds, and economical constraints, such as power-consumption for high-speed packet processing interfaces. Although more advances of technologies may resolve the limitation of packet processing capacity and reduce the cost, the above-mentioned characteristics are essential for the packet-switching paradigm.

Thus, constructing only packet switched network or circuit switched network cannot satisfy requirements, such as the high reliability and large bandwidth, for future networking services. An integration of circuit switched network and packet switched network is required to enjoy strength of both circuit-switching paradigm and packet-switching paradigm. One possible approach to fulfill this is to deploy the WDM technology and allocate different wavelengths for each network. Hereafter, we will call a network based on the packet-switching paradigm as the packet-based network and call a network based on the circuit-switching paradigm as the path-based network.

We have investigated a performance of path/packet integrated networks in [5], [6]. Reference [5] evaluates the performance of path/packet integrated networks with respect to the network throughput, and shows the advantage of path/packet integrated networks. The authors developed a numerical method that derives the network throughput with a fixed wavelength allocation for packet-based network and path-based network. Reference [6] demonstrates that the fixed wavelength allocation does not minimize the latency, which is defined from when a data transfer request arises to when the data transfer completes, when the network environments changes. The simulation results clearly show that the optimal wavelength allocation depends on the arrival rate of data transfer requests, so the authors propose a dynamic wavelength allocation method that is based on a threshold of queue length of buffer in the packet-based network.

In this paper, we present another dynamic wavelength

allocation method that is based on a biological symbiosis model developed in [7]. The biological symbiosis model is a mathematical model that explains co-existing and co-working of two types of bacterial strains. By interpreting bacterial strains as the amount of traffic transferred by packet-switched / circuit-switched networks, we achieve the co-existing and co-working of packet-switched / circuit-switched networks against the changes of network conditions.

This paper is organized as follows. In Section 2, we introduce the network architecture of path/packet integrated networks. In Section 3, we explain our biologically-inspired wavelength allocation method. Section 4 evaluates the performance in path/packet integrated networks. Section 5 concludes this paper.

II. A MODEL OF PATH/PACKET INTEGRATED NETWORK

Each node in path/packet integrated network consists of IP router and OXC connected by optical fibers.

The path/packet integrated network provides a packet switched network and a circuit switched network by allocating wavelengths for each network. For the packet switched network, the virtual network topology is constructed by configuring a set of lightpaths based on a long-term measurement of traffic volume. When a packet arrives at a node, the packet is forwarded to the next node in the VNT. In the circuit switched network, when a data transfer request arises, lightpaths are established between source and destination nodes on-demand basis (Figure 1). RSVP-based wavelength reservation protocol is used in this paper.

Each end-host connecting with the node has two network interfaces; one for inject IP packets into the packet switched network and one for establish a lightpath between two end-hosts. When the data transfer request arises, the end-host selects the packet switched network or the circuit switched network to transfer the data. Various strategies to select the network can be considered. We believe that the optimal strategy highly depends on the traffic characteristics, so the highly sophisticated strategy may be necessary. Instead of chasing the sophisticated strategy, we take a simple strategy to select the network because our primary concern of the current paper is to develop an adaptive wavelength allocation method. In this paper, the sender host first tries to transfer the data in circuit switched network. When the lightpath establishment succeeds, the sender host transfers the data with the transmission capacity of wavelengths. When the lightpath establishment fails, the sender host gives up transferring the data via circuit switched network and transfers the data via the packet switched network. In this case, the sender host uses a TCP protocol for the data transfer.

We consider the dynamic wavelength allocation for packet-switched network and circuit-switched network. Its enabling architecture is illustrated in Figure 2. There is a controller to manage the configuration of OXCs and observe the network environment, such as the buffer utilization of IP routers, the blocking rate of lightpath establishments, and the packet dropped rate in the IP router. Depending on the wavelength methods explained in later, the controller collects information on the buffer utilization of IP router (in threshold-base wavelength allocation) or the blocking rate and the packet drop rate in the IP router (in biologically-inspired wavelength allocation). Then, for example, when the controller determines to increase the amount of wavelengths allocated to the path switching plane, the controller immediately reconfigures the optical switch (e.g., λ_3 in Fig. 2) so as not to forward the optical-signal to the IP router.

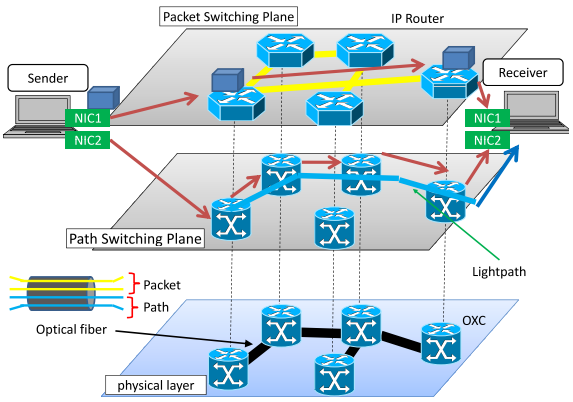

Fig. 1. A network architecture

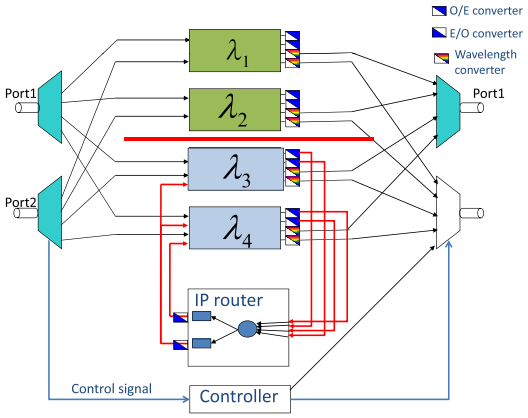

Fig. 2. A node architecture for dynamic wavelength allocation; Focusing on the output port 1. Two wavelengths are assigned for packet switching plane and path switching plane.

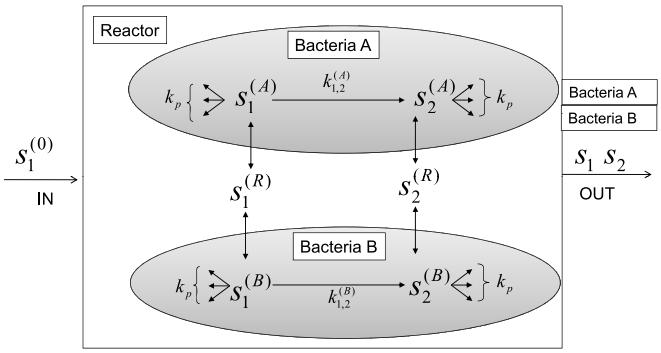

Fig. 3. Biological symbiosis model

TABLE I
CORRESPONDENCE TABLE BETWEEN PARAMETERS IN BIOLOGICAL SYMBIOSIS MODEL AND OUR DYNAMIC WAVELENGTH ALLOCATION METHOD

$X^{(A)}$	Number of wavelengths allocated to the path switching plane	$X^{(B)}$	Number of wavelengths allocated to the packet switching plane
$s_1^{(A)}$	Number of wavelengths allocated to the path switching plane per unit of time	$s_1^{(B)}$	Number of wavelengths allocated to the packet switching plane per unit of time
$s_2^{(A)}$	Throughput in the path switching plane per unit of time [Gbps]	$s_2^{(B)}$	Throughput in the packet switching plane per unit of time [Gbps]
$k_{1,2}^{(A)}$	Throughput of the path switching plane [Gbps]	$k_{1,2}^{(B)}$	Throughput of the packet switching plane [Gbps]
$u^{(A)}$	Growth rate of the path switching plane per unit of time	$u^{(B)}$	Growth rate of the packet switching plane per unit of time
$s_1^{(R)}$	Internal variable that represents the remaining wavelength resources that are not assigned to switching planes	$s_2^{(R)}$	Internal variable that represents throughput per unit of time [Gbps]
$s_1^{(0)}$	Number of wavelength multiplexed on a fiber	$s_2^{(0)}$	Parameter (set to 0)
$k^{(p)}$	Parameter	D	Parameter
P	Parameter	α	Parameter

III. BIOLOGICALLY-INSPIRED WAVELENGTH ALLOCATION METHOD

A. Biological symbiosis model

In [7], the authors proposed a mathematical model of a mechanism that permitted two types of bacterial strains to live together by exchanging metabolites through a reactor. Bacterial strains have a metabolic network of generating metabolite S_2 from other metabolite S_1. Metabolites diffuse in and diffuse out of a cell through membrane depending on the difference in metabolic concentrations (Figure 3). The dynamics of concentrations of metabolites in a cell of strain A and B are formulated as,

$$\begin{aligned} ds_1^{(A)}/dt &= (P/V)(s_1^{(R)} - s_1^{(A)}) - (k_{1,2}^{(A)} + k_p)s_1^{(A)}, \\ ds_1^{(B)}/dt &= (P/V)(s_1^{(R)} - s_1^{(B)}) - (k_{1,2}^{(B)} + k_p)s_1^{(B)}, \\ ds_2^{(A)}/dt &= (P/V)(s_2^{(R)} - s_2^{(A)}) + k_{1,2}^{(A)} s_1^{(A)} - k_p s_2^{(A)}, \\ ds_2^{(B)}/dt &= (P/V)(s_2^{(R)} - s_2^{(B)}) + k_{1,2}^{(B)} s_1^{(B)} - k_p s_2^{(B)}, \end{aligned}$$

where P stands for the permeation coefficient of cell membrane, V does for the average volume of a cell. $s_{1,2}^{(A)}$, $s_{1,2}^{(B)}$ and $s_{1,2}^{(R)}$ are metabolite concentrations in a cell of strain A and B in the reactor, respectively. k_p is the metabolite consumption rate in a cell. $k_{1,2}^{(A)}$ and $k_{1,2}^{(B)}$ are the metabolite conversion rate in a cell of strain A and B. Next, metabolite concentrations in the reactor evolve as,

$$\begin{aligned} ds_1^{(R)}/dt &= D(s_1^{(0)} - s_1^{(R)}) + X^{(A)}P(s_1^{(A)} - s_1^{(R)}) \\ &\quad + X^{(B)}P(s_1^{(B)} - s_1^{(R)}), \\ ds_2^{(R)}/dt &= D(s_2^{(0)} - s_2^{(R)}) + X^{(A)}P(s_2^{(A)} - s_2^{(R)}) \\ &\quad + X^{(B)}P(s_2^{(B)} - s_2^{(R)}), \end{aligned}$$

where $X^{(A)}$ and $X^{(B)}$ stand for the number of cells of strain A and B per volume in the reactor. The fresh medium containing metabolites of concentration $s_1^{(0)}$ and $s_2^{(0)}$ are added to the reactor at the constant rate and the culture is drained at the same rate. D means the resultant dilution rate. Change in population of cells is formulated as,

$$\begin{aligned} dX^{(A)}/dt &= u^{(A)}X^{(A)} - DX^{(A)}, \\ dX^{(B)}/dt &= u^{(B)}X^{(B)} - DX^{(B)}, \end{aligned}$$

where the growth rate $u^{(A)}$ and $u^{(B)}$ is defined as,

$$\begin{aligned} u^{(A)} &= \alpha s_1^{(A)} s_2^{(A)}, \\ u^{(B)} &= \alpha s_1^{(B)} s_2^{(B)}, \end{aligned} \tag{1}$$

Eq. (1) implies that a cell with high metabolite concentration grows fast. Here, α (> 0) is a constant value.

B. Applying the biological symbiosis model to dynamic wavelength allocation method

In this section, we explain how the biological symbiosis model can be applied to the wavelength allocation methods. More specifically, we describe how to determine the amount of wavelengths allocated for the packet switching plane and the path switching plane. Since the biological symbiosis model does not distinguish the role of A and B, we regard the bacteria A for the path switching plane and the bacteria B for the packet switching Table.

plane I is the correspondence table between parameters in biological symbiosis model and our wavelength allocation method. The number of bacteria A, $X^{(A)}$, represents the number of wavelengths allocated to the path switching plane and the number of bacteria B, $X^{(B)}$, represents the number of wavelengths allocated to the packet switching plane. In calculating $X^{(A)}$ and $X^{(B)}$, we need to specify definitions of $k_{1,2}^{(A)}$ and $k_{1,2}^{(B)}$ since they represent degree of productivity of the path switching plane and the packet switching plane. In our model, the degree of productivity is derived from the throughput of each plane, that is, $k_{1,2}^{(A)}$ and $k_{1,2}^{(B)}$ is calculated from following equations,

$$k_{1,2}^{(A)} = (1.0 - P_b) \cdot C, \tag{2}$$

$$k_{1,2}^{(B)} = (s/RTT) \cdot \sqrt{(3/2)} \cdot \sqrt{(1/p)}, \tag{3}$$

where P_b is the blocking rate of lightpath establishments on the path switching plane and C is the bandwidth of lightpaths (in [Gbps]). B is the packet size and RTT is the propagation delay of connections. p is the packet loss probability in the packet switching plane. β is the parameter that adjusts the throughput by [Gbps] and is set to 10^{-9}. Note that $k_{1,2}^{(B)}$ is derived from a TCP's throughput calculation formula and RTT should be determined by the observed round-trip time. In more realistic scenarios, we may need the RTT estimation at the controller [8]. However, in our simulation, RTT is set to the propagation delay because the queuing delay is relatively small in the WDM-based networks.

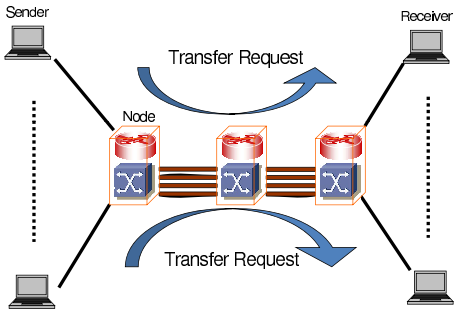

Fig. 4. Dumbbell network

TABLE II
SIMULATION PARAMETERS

OD pairs	120
Link propagation delay	10 ms
Arrival process	Poisson
Amount of data	Exponential distribution with mean 1 Gbit
Bandwidth of a wavelength	10 Gbps
Number of wavelengths	8
Buffer size at IP routers	256 MB

IV. EVALUATION

A. Simulation parameters

For our evaluation, we use the dumbbell network depicted in Figure 4. The network has sender hosts and receiver hosts each of which equips with two network interfaces. Nodes, each having IP router and OXC, are connected with hosts via the network interfaces, and are also connected with each other via WDM transmission link. The number of wavelengths multiplexed between nodes is eight, and the buffer size of each IP router is 256MB. In this evaluation, we assume that the bandwidth of links between sender hosts and nodes is enough not to be a bottleneck of path/packet integrated networks. We also assume that there is no OXC configuration delay, that is, the lightpath setup delay is determined solely by the propagation delay.

In the packet switching plane, the packet is processed based on the FIFO (First-in First-out) drop-tail discipline. The sender host employs TCP Reno when the data is transferred via the packet switching plane. When the path switching plane is used, the sender host transfers the data with the transmission capacity of wavelengths since the sender host exclusively uses the lightpath. The other simulation parameters are summarized in Table II.

The performance metric used in this paper is the average latency. We define the latency as the time from when a data transfer request arises to when the data transfer completes. The formal definition of the average latency is,

$$(\sum_{i=1}^{n_c} P_i + \sum_{k=1}^{n_p} B_k + \sum_{k=1}^{n_p} T_k)/(n_c + n_p), \quad (4)$$

where n_c is the number of data transfers completed by using the path switching plane and n_p is the number of data transfers completed by using the packet switching plane. P_i represents the latency of the i-th request among the n_c requests. For the k-th request among the n_p requests, we define B_k as the time consumed for exchanging the control messages to establish a lightpath and define T_k as the time from when a TCP session starts to when the data transfer completes.

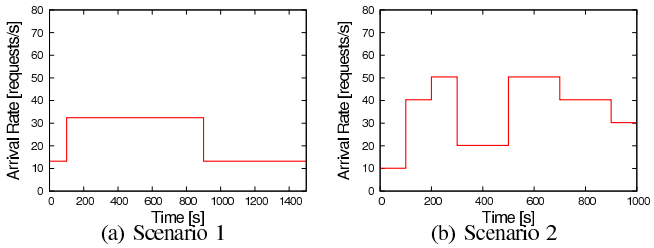

(a) Scenario 1 (b) Scenario 2

Fig. 5. Arrival rate for two traffic scenarios

For the biologically-inspired wavelength allocation method, we set the parameters to be $k^{(P)} = 1$, $D = 0.7$, $P = 1$, $\alpha = 1$, and $S_1^{(0)} = 8$. For the arrivals of data transfer requests, we prepare two scenarios:

1) Arrival rate of data transfer request is set to be 13.2 request/s for [0s-100s, 900-1500s], and increase the arrival rate to be 32.4 requests/s for [100s -900s] (Figure 5(a));
2) Arrival rate is set to $\beta \times 10.1$ request/s . The β is the integer number between 1 to 5 and is selected randomly for every 100s. Resulting arrival rate depending on the time is shown in Figure 5(b).

For comparison purpose, we prepare the fixed wavelength allocation with seven wavelengths for the path switching plane and one wavelength for the packet switching plane. In addition, we prepare the pre-calculated wavelength allocation (denote "pre-calculated") by assuming that the arrival rate is known beforehand. Given the arrival rate, we conduct the simulation and calculate the optimal wavelength allocation that achieves minimum latency. Note that "pre-calculated" changes the wavelength allocation based on the changes of arrival rate, not based on the current network conditions such as buffer utilization and/or blocking rate of lightpath establishments. We also uses threshold-based wavelength allocation method presented in [6]. In the threshold-based method, the average queue length of buffer is retrieved every 30 seconds, while the biologically-inspired wavelength allocation method updates the values of equations at every second.

B. Simulation results and discussions

TABLE III
LATENCY BY WAVELENGTH ALLOCATION METHODS: SCENARIO 1

	Fixed	Threshold	Pre-calculated	Biologically-inspired
Latency [ms] (overall)	6407	3645	2409	2577
Latency [ms] (packet switching plane)	25133	14979	8871	9480

1) Scenario 1: Figure 6 shows the actual queue length of the buffer in the IP router. We observe that the queue length with threshold-based wavelength allocation method and

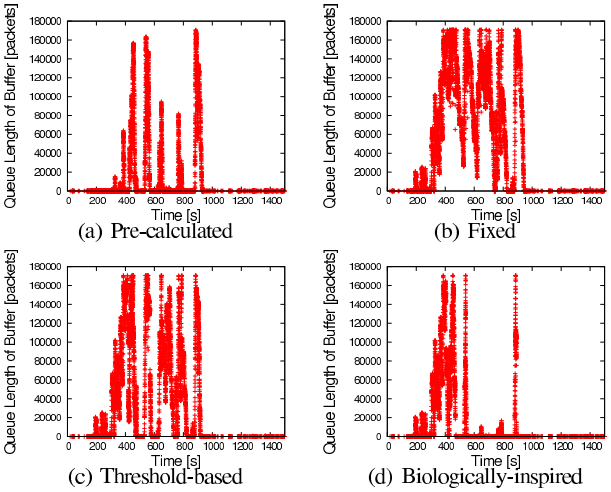

(a) Pre-calculated (b) Fixed

(c) Threshold-based (d) Biologically-inspired

Fig. 6. Queue length at IP routers: Scenario 1

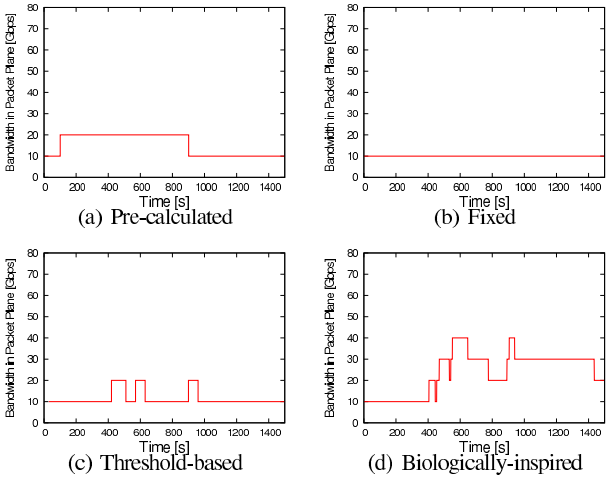

(a) Pre-calculated (b) Fixed

(c) Threshold-based (d) Biologically-inspired

Fig. 7. Bandwidth allocated to the packet switching plane : Scenario 1

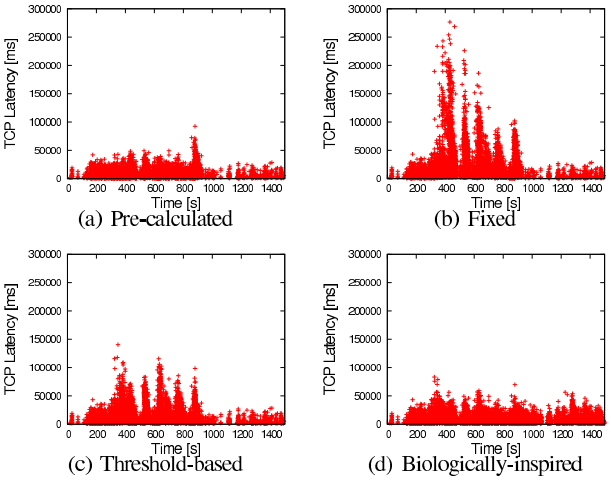

(a) Pre-calculated (b) Fixed

(c) Threshold-based (d) Biologically-inspired

Fig. 8. Latency of TCP connections : Scenario 1

biologically-inspired wavelength allocation method is less than that with the fixed wavelength allocation method (Fig 6(a)) . The queue length with the pre-calculated wavelength allocation (Fig 6(a)) is less than the biologically-inspired wavelength

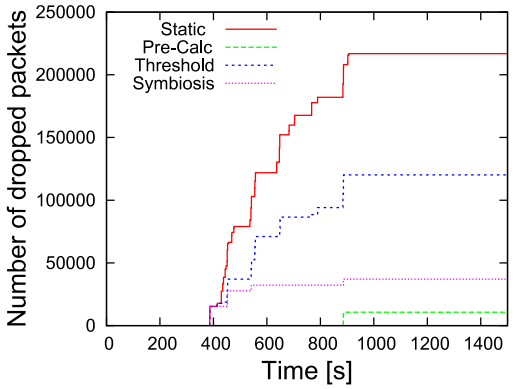

Fig. 9. Accumulated number of dropped packets: Scenario 1

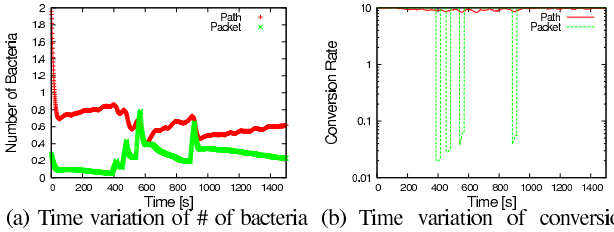

(a) Time variation of # of bacteria (b) Time variation of conversion rate

Fig. 10. Behaviors of our biological symbiosis model : Scenario 1

allocation method, but the difference is marginal. To see how four wavelength allocation methods work, we show the time variation of bandwidth allocated for the packet switching plane in Figure 7. Both the threshold-based wavelength allocation method (Figure 7(c)) and the biologically-inspired wavelength allocation method (Figure 7(d)) adaptively changes the bandwidth for the packet switching plane. The bandwidth allocation of biologically-inspired wavelength allocation is close to the pre-calculated wavelength allocation.

Figure 8 shows the latency of TCP connections that are transferred through the packet switching plane. X-axis represents the time when a TCP connection finishes and Y-axis represent the latency of the TCP connection. Since the threshold-based and biologically-inspired wavelength allocation method decreases the average queue length during the higher arrival rate, the latency of TCP connection is greatly reduced, which in turn decreases the average latency in the path/packet integrated networks.

Figure 9 shows the accumulated number of dropped packets for each wavelength allocation method. Note that no packet loss occurs in the case of the pre-calculated wavelength allocation. The biologically-inspired wavelength allocation method takes the second smallest number of packet loss.

We next investigate the biologically-inspired wavelength allocation method in detail. To understand the behaviors of biologically-inspired wavelength allocation method, we show the time variation of number of bacteria in Figure 10(a) and the conversion rate in Figure 10(b). We observe that when the conversion rate in the packet switching plane is drastically decreased, the number of bacteria that corresponds to the path switching plane is drastically increased. This is because the biological symbiosis model allocates the wavelength resources

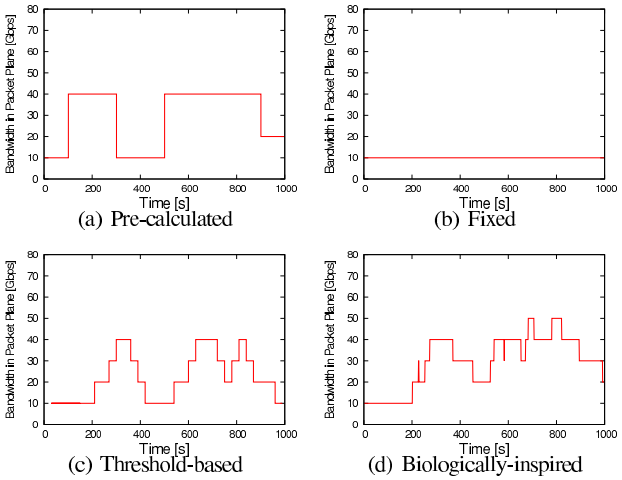

Fig. 11. Bandwidth allocated to the packet switching plane : Scenario 2

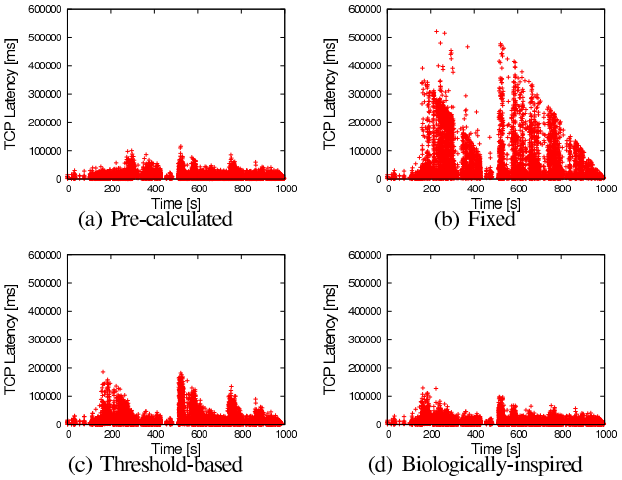

Fig. 12. Latency of TCP connections : Scenario 2

effectively when the traffic load on the path switching plane and the packet switching plane is not balanced. Table III shows the overall latency in path/packet integrated networks and the latency of data transfers that uses the packet switching plane. Note that when the lightpath establishment succeeds, the latency is around 180 [ms] since the data transfer time with the bandwidth of lightpath. From Table III, we observe that the biologically-inspired wavelength allocation method makes the latency to be low.

2) Scenario 2: The arrival rate used in Scenario 2 is shown in Figure 5(b). We first show the results of bandwidth allocated for the packet switching plane (Figure 11), latency of TCP connections (Figure 12), and accumulated number of dropped packets (Figure 13). The simulation results of Scenario 2 are almost the same as the simulation results of Scenario 1; the biologically-inspired wavelength allocation method makes latency low. These results show that the biologically-inspired wavelength allocation model achieves adaptive wavelength allocation against the changes of network environments.

V. Conclusion

The main advantage of the path/packet integration is to enjoy strengths of both packet switching paradigm and circuit switching paradigm. However, depending on the network condition, the amount of wavelengths allocated for networks should be changed to achieve the minimum latency. In this paper, we developed a biologically-inspired wavelength allocation method that dynamically allocates wavelengths to path/packet integrated networks. Our method is based on a biological symbiosis model that explains co-existing and co-working of two types of bacterial strains in biological systems. The results showed that biologically-inspired wavelength allocation method achieves a nearly 40% reduction of the latency from threshold-based dynamic wavelength allocation method.

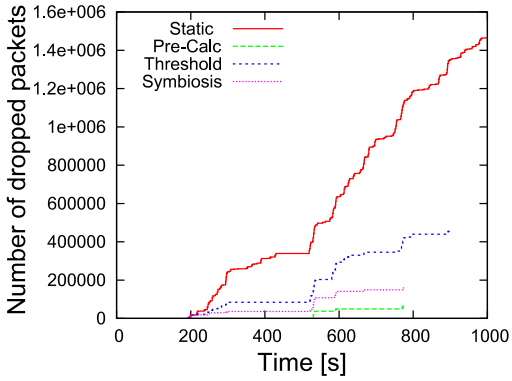

Fig. 13. Accumulated number of dropped packets: Scenario 2

TABLE IV
Latency by wavelength allocation methods: Scenario 2

	Fixed	Threshold	Pre-calculated	Biologically-inspired
Latency [ms] (overall)	14731	7462	5124	4789
Latency [ms] (packet switching plane)	53856	16723	9064	9974

Acknowledgement

This work was supported in part by the National Institute of Information and Communications Technology (NICT).

References

[1] H. Zang, J. P. Jue, L. Sahasrabuddhe, R. Ramamurthy, and B. Mukherjee, "Dynamic lightpath establishment in wavelength-routed WDM networks," *IEEE Communications Magazine*, pp. 100–108, Sept. 2001.

[2] M. Kodialanm and T. V. Lakshman, "Intergrated dynamic IP and wavelength routing in IP over WDM networks," in *Proceedings of IEEE INFOCOM*, pp. 358–366, Apr. 2001.

[3] M. Veeraraghavan, X. Zheng, W. Feng, H. Lee, E. K. Chong, and H. Li, "Scheduling and transport for file transfers on high-speed optical circuits," *Journal of Grid Computing*, vol. 1, pp. 395–405, Dec. 2003.

[4] S. Lin and N. McKeown, "A simulation study of IP switching," in *Proceedings of ACM SIGMCOM1997*, pp. 15–24, Sept. 1997.

[5] M. Ohashi, S. Arakawa, and M. Murata, "Performamnce analysis of packet/path integrated architecture on wdm-based networks," *Technical Report of IEICE* (PN2007-73), vol. 107, pp. 1–6, Mar. 2008.

[6] N. Tsutsui, S. Arakawa, and M. Murata, "Latency evaluation of WDM-based packet/path integrated networks," in *Proceedings of The Sixth International Conference on Networking and Services (ICAS)*, Mar. 2010.

[7] T. Yomo, W.-Z. Xu, and I. Urabe, "Mathematical model allowing the coexistence of closely related competitors at the initial stage of evolution," *Researched on Population Elocogy*, vol. 38, no. 2, pp. 239–247, 1996.

[8] H. Jiang and C. Dovrolis, "Passive estimation of TCP round-trip times," *ACM SIGCOMM Computer Communication Review*, vol. 32, pp. 75–88, July 2002.